



Entropy models for the description of the solid–liquid regime of deep eutectic solutions

Laura J.B.M. Kollau^{a, b, c}, Mark Vis^{a, b, c, *}, Adriaan van den Bruinhorst^{a, b, c},
Remco Tuinier^{a, b, d}, Gijsbertus de With^a

^aLaboratory of Physical Chemistry, Department of Chemical Engineering and Chemistry, Eindhoven University of Technology, the Netherlands

^bInstitute for Complex Molecular Systems, Eindhoven University of Technology, the Netherlands

^cLaboratoire de Chimie, Ecole Normale Supérieure de Lyon, France

^dVan 't Hoff Laboratory for Physical and Colloid Chemistry, Debye Institute for Nanomaterials Science, Utrecht University, the Netherlands

ARTICLE INFO

Article history:

Received 9 September 2019

Received in revised form 8 November 2019

Accepted 16 November 2019

Available online 20 November 2019

Keywords:

Deep eutectic solvents

Thermodynamics

Phase diagrams

Entropy

Melting point depression

ABSTRACT

A necessary prerequisite for applying deep eutectic solutions (DESs) is to understand the phase behavior and to be able to quantify the liquid window of these mixtures. The non-ideality of the phase behavior is determined by the contributions of excess entropy and enthalpy. While the total Gibbs energy of mixing can be inferred from the solid–liquid phase behavior, the entropic and enthalpic contributions can not be distinguished. Hence, by assuming ideal mixing entropy, all excess free energy is captured as an enthalpic contribution. The ideal mixing entropy provides a reasonable description when the components are similar in size and shape. This is not always the case for the components typically used in DESs. Here, the suitability of two non-ideal entropy models is investigated, aiming to describe the phase behavior of DESs more accurately. First, by using Flory–Huggins entropy accounting for the different molar volumes of the components, we show that ideal entropy of mixing underestimates the entropic contribution for mixtures of components often used for DESs. The value of molar volume employed has a significant influence on the resulting entropy of mixing and thus on the resulting enthalpy. Second, correcting for the molar area as well, using the Staverman–Guggenheim entropy, appears to have negligible impact for the compounds considered. Both the use of a non-ideal mixing entropy and the specific choice of the molar volume significantly affect the obtained enthalpy of mixing and will thus alter the interaction parameters, obtained using a Redlich–Kister-like mixing enthalpy, as compared to models based on ideal mixing entropy.

© 2019 The Authors. Published by Elsevier B.V. This is an open access article under the CC BY-NC-ND license (<http://creativecommons.org/licenses/by-nc-nd/4.0/>).

1. Introduction

In 1884 Frederick Guthrie [1] coined the term eutectic by combining the Greek words ‘εύ’—meaning good/easy—with ‘τήκεω’—which means melting—and defined it as:

“(…) bodies made up of two or more constituents, which constituents are in such proportion to one another as to give the resultant compound body a minimum temperature of liquefaction—that is, a lower temperature of liquefaction than that given by any other proportion.”

Following this, Guthrie connected solubility to melting [2]:

“The phenomenon of fusion per se is continuous with, and nothing more than an extreme case of, liquefaction by solution. (...) Hence

the question, is this a case of fusion or solution is to be answered by the reply, it is continuous with both.”

At the beginning of this century the term ‘deep eutectic solvents’ was first used [3] for a mixture of two components showing eutexia in an extreme form: a remarkably large melting point depression. This results for instance in a liquid binary mixture made from components, which are by themselves solid at room temperature. It was shown that this feature could be extended to other mixtures of similar constituents resulting in mixtures with tuneable physical properties. With this, the potential of these mixtures as designer solvents was founded, considering that their properties can be tailored based on the nature of its constituents. Hence, it is not a surprise that since the term DES was introduced, numerous studies on the properties of these mixtures were performed, postulating applications for solvents like biomass processing [4–7], CO₂ capture [8, 9] and many others [10–12]. It should be noted that even though DESs are often treated as a new class of solvents [13], eutectic mixtures were applied widely

* Corresponding author at: Laboratory of Physical Chemistry, Department of Chemical Engineering and Chemistry, Eindhoven University of Technology, the Netherlands.
E-mail address: m.vis@tue.nl (M. Vis).

already as pharmaceuticals in order to solubilize or liquefy specific compounds [14–18], as phase change material [19–26], and in liquid crystals [27–30].

1.1. The solubility limits of non-ideal eutectic mixtures

Phase diagrams describe the phase behavior and are essential when designing industrial products and processes. Understanding the phase behavior is needed to be able to quantify the solid–liquid coexistence as a function of composition, which provides the melting point depression, and to shed light on the liquid window of these mixtures. However, little work is yet directed towards phase diagrams and/or the relation between the melting point depressions of eutectic mixtures with large melting point depressions and the properties of its constituents.

The aim here is to describe the molar Gibbs energy of mixing g and to differentiate between the contributions resulting from entropy s and enthalpy h :

$$g = h - Ts \quad (1)$$

where g can directly be related to experimentally obtained solid–liquid phase diagrams as follows. Since g is the molar free energy of mixing, the change $\Delta\mu_i(x_i)$ in chemical potential due to mixing for component i as a function of mole fraction x_i follows as:

$$\left(\frac{\partial ng}{\partial n_i}\right)_{p,T,n_{j \neq i}} = \Delta\mu_i(x_i) = RT \ln a_i, \quad (2)$$

where n_i is the number of moles of component i , $n = \sum_i n_i$, a_i is the activity, and $\Delta\mu_i(x_i) = \mu_i(x_i) - \mu_i^*$. The change $\Delta\mu_i(x_i)$ in chemical potential is in turn related to the melting point T of the mixture according to:

$$\frac{\Delta\mu_i(x_i)}{RT} = \frac{\Delta H_i}{R} \left(\frac{1}{T_i^*} - \frac{1}{T} \right). \quad (3)$$

Here the enthalpy of fusion ΔH_i is assumed to be independent of temperature and T_i^* is the melting point of the pure component.

For ideal mixtures the melting point depression originates from an increase in configurations—i.e., entropy—when mixing components in the liquid state. In this case the enthalpy $h = h^{\text{id}} = 0$ resulting in:

$$g = g^{\text{id}} = -Ts^{\text{id}}. \quad (4)$$

For s^{id} one generally uses the Gibbs entropy, which results from Boltzmann's equation comprising the probability of the number of microstates in a mixture, i.e. the number of complexions, yielding:

$$\frac{g^{\text{id}}}{RT} = \sum_i x_i \ln x_i. \quad (5)$$

which results, via Eq. (2), in an expression for $\Delta\mu_i$, which reads:

$$\frac{\Delta\mu_i}{RT} = \ln x_i. \quad (6)$$

Generally, however, there is a need to account for enthalpic interactions when describing deep eutectic mixtures. Enthalpic

interactions can be included using excess functions for the Gibbs energy g^e defined by:

$$g = g^{\text{id}} + g^e. \quad (7)$$

For example, for a binary mixture, regular solution theory [31], where the enthalpic contributions can be quantified using one interaction parameter χ , leads to:

$$\frac{h^e}{RT} = \chi x_1 x_2. \quad (8)$$

We showed [32] that the description of the phase boundaries can be improved when Eq. (8) is expanded using an orthogonal Redlich–Kister-like polynomial [33–36]:

$$\frac{h^e}{RT} = x_1 x_2 [p_0 + p_1 \mathcal{P}_1(x_1 - x_2) + p_2 \mathcal{P}_2(x_1 - x_2) + \dots], \quad (9)$$

where $\mathcal{P}_k(x_1 - x_2)$ is the Legendre polynomial of order k as a function of the variable $x_1 - x_2$. Terminating the expansion after first order, using $\mathcal{P}_1(x_1 - x_2) = x_1 - x_2$,

$$\frac{h^e}{RT} = x_1 x_2 [p_0 + p_1(x_1 - x_2)] \quad (10)$$

was found to yield a description at least as good as a commonly used thermodynamic engineering model to describe two-phase equilibria, namely non-random two-liquid theory (NRTL) [37–40]. The advantage of using the orthogonal Redlich–Kister-like polynomial rather than NRTL is that the zeroth order parameter p_0 can be identified still as the χ parameter of regular solution theory and that its value is unaffected by the addition of the orthogonal higher order terms. Thus, higher order terms can be added when this is statistically justified, while not affecting the physical interpretation of regular solution theory. In this work we employ the first order expansion, Eq. (10), but if the addition of the first order term does not statistically improve the fit of the phase diagram, we set $p_1 = 0$ [32], thus essentially using Eq. (8).

As a direct result from using the ideal Gibbs entropy s^{id} all the excess free energy is captured effectively as an enthalpic contribution. The ideal mixing entropy s^{id} provides a reasonable description for the number of complexions when the components are similar in size and shape. This is, of course, far from the actual situation for the components typically used in DESS. Here both the volumes as well as the surface areas of the components may differ to a smaller or larger extent.

To get a better understanding of the enthalpic interactions resulting in the melting point depressions observed, we employ here different entropy models in order to isolate the enthalpic contributions as much as possible. We compare the following entropy models for binary mixtures in this work. First, the mole fraction-based ideal Gibbs entropy s^{id} —now labelled as s^x —is used as reference, Eq. (11a). Second, we use the non-ideal volume fraction-based entropy model from Flory–Huggins theory, s^ϕ , Eq. (11b). As a third, we employ the Staverman–Guggenheim correction s^θ , Eq. (11c), which also takes surface area in account:

$$s^x = x_1 \ln x_1 + x_2 \ln x_2, \quad (11a)$$

$$s^\phi = x_1 \ln \phi_1 + x_2 \ln \phi_2, \quad (11b)$$

$$s^\theta = x_1 \ln \phi_1 + x_1 Q_1 \ln \left(\frac{\theta_1}{\phi_1} \right) + x_2 \ln \phi_2 + x_2 Q_2 \ln \left(\frac{\theta_2}{\phi_2} \right). \quad (11c)$$

Here ϕ and θ denote the volume fraction and surface fraction, defined by:

$$\phi_i(x_i) = \frac{x_i V_{m,i}}{\sum_j x_j V_{m,j}}, \quad (12)$$

$$\theta(x_i) = \frac{x_i A_{m,i}}{\sum_j x_j A_{m,j}}, \quad (13)$$

where we take $V_{m,i}$ as the van der Waals molecular volume for component i and $A_{m,i}$ as the van der Waals molecular surface area for component i . Further, Q_i is a direct function of ϕ_i and θ_i [41]:

$$Q_i = \frac{1 - \frac{\phi_i}{x_i}}{1 - \frac{\theta_i}{x_i}}. \quad (14)$$

1.1.1. Flory–Huggins entropy of mixing

The Flory–Huggins entropy of mixing accounts for unequally sized molecules and results in the following expression for the change in chemical potential upon mixing:

$$\frac{\Delta\mu_i}{RT} = \ln \phi_i + \left(1 - \frac{\phi_i}{x_i}\right). \quad (15)$$

From this expression it follows that ideal mixing entropy is only achieved in case of equal molar volumes of both components. The molar volumes (based on different methods, see experimental section) as well as the other relevant fusion properties of the components used in this work are listed in Table 1.

The effect of a difference in molecular volumes on the liquidus is schematically depicted in Fig. 1. In panel I solid–liquid equilibria based on the ideal mixing entropy using identical fusion properties are depicted as dashed curves. This results in a fully symmetrical phase diagram. The phase boundaries resulting from a mixing entropy when the molar volume of component B is larger than component A are plotted in panel II as the dashed curves. The solid curves demonstrate the influence of a negative mixing enthalpy, Eq. (8) with $\chi < 0$, on the phase behavior. Overall, both a difference in molar volumes as well as binary attractions lead to a decrease of the eutectic temperature.

1.1.2. Staverman–Guggenheim entropy of mixing

Guggenheim [42] showed that the Flory–Huggins model overestimates the entropy of mixing, because the connectivity of sites in a molecule reduces the number of possible configurations, and derived a correction term. Staverman [43] essentially derived the

same expression and applied it to more complicated molecules. The expression for the change in chemical potential upon mixing is:

$$\frac{\Delta\mu_i}{RT} = \ln \phi_i - Q_i \ln \left(\frac{\phi_i}{\theta_i}\right). \quad (16)$$

The relevant experimental parameters are listed in Table 1.

Panel III in Fig. 1 shows a slightly higher eutectic temperature for this entropy model compared to the Flory–Huggins entropy in panel II. The Staverman–Guggenheim model contains, besides the molecular and volume fraction, the surface fraction and requires as additional parameter the number of nearest neighbors for each compound. Recently Krooshof et al. showed that the number of nearest neighbors is directly related to the molar, volume, and surface fraction through Eq. (14), which enables to further simplify the expressions [41].

1.1.3. Model systems

The systems used here to demonstrate the different entropy models are mixtures of the salt tetrapentylammonium bromide (Pe_4NBr) with erythritol, succinic acid, and pimelic acid, see Fig. 2. The selected binary mixtures differ in one component and non-ideality. This allows for the evaluation of the suitability of the described thermodynamic models for DESs with different effective strengths of interaction. We have previously published detailed phase diagrams for these mixtures elsewhere and will reuse that information for this work [32]. The earlier obtained interaction parameters, based on ideal mixing entropy, suggest attractions for the mixtures of Pe_4NBr in the order pimelic acid > succinic acid > erythritol [32].

2. Results and discussion

The results for the mixture of erythritol with Pe_4NBr are displayed in Fig. 3 and listed in Table 2. Fig. 3 panel I displays the entropy of mixing s of the mixture versus the composition x . It clearly illustrates the difference between the models for the calculation of s . It shows that the Gibbs entropy of mixing s^x is smaller than the Flory–Huggins estimation for the entropy of mixing s^{ϕ} . It appears that the differences in available surface between the components, Staverman–Guggenheim entropy of mixing s^{θ} are too small to produce significant differences in entropy, and it is not necessary to take these into account when describing the phase behavior.

What is remarkable, though, is that the precise value of the molar volume used has a significant influence on the resulting entropy of mixing. Here we considered molar van der Waals volumes resulting from the Molecular Modeling Pro software s_{MMP}^j , and molar van der Waals volumes from an empirical correlation with molar volumes based on Bondi's estimates for the van der Waals volume s_{Bondi}^j [44]. The values used for the volumes as well as the surfaces are listed in Table 1. Somewhat surprisingly, as both methods intend to estimate the van der Waals volume, not only the absolute values differ but also the ratios between the components. This causes the entropy to differ,

Table 1

Melting point T^* , enthalpy of fusion ΔH , molar volume V_m , and molar surface A_m of individual components.

Component	T^* [K]		ΔH [J mol ⁻¹]		V_m [cm ³ mol ⁻¹]		A_m [10 ⁹ cm ² mol ⁻¹]	
	a		a		b	c	b	c
Erythritol	394.7		39,300.7	83.7	46.4	67.4	11.7	9.9
Succinic acid	460.0		37,105.1	75.7	41.9	60.5	10.6	8.8
Pimelic acid	378.5		26,074.0	120.0	66.5	90.1	16.5	12.8
Pe_4NBr	375.9		40,140.5	344.2	190.7	234.8	46.2	33.4

^a Measured experimentally.

^b Estimated van der Waals volume/area according to Bondi [44].

^c Estimated van der Waals volume/area according to Molecular Modeling Pro software.

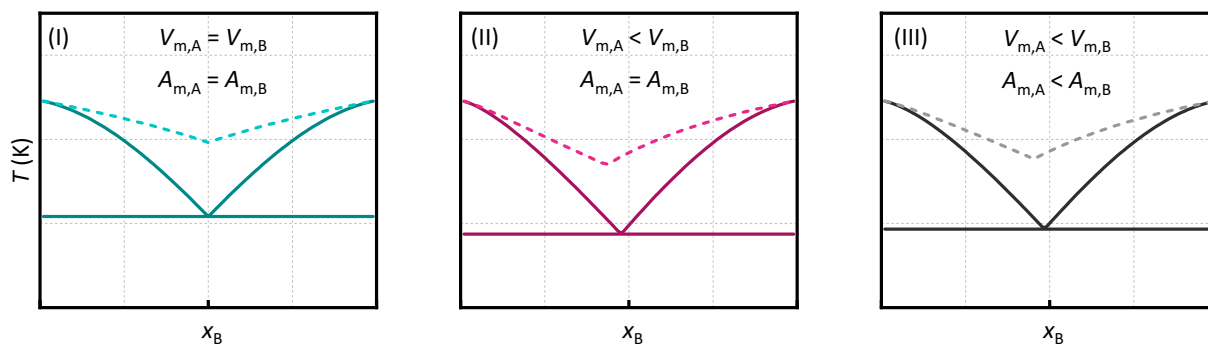


Fig. 1. Schematic illustrations of the effect of molecular volume and surface on symmetrical eutectic phase behavior: (I) Symmetric phase diagrams where both components have identical molecular volumes (V_m) and surfaces (A_m). (II) The influence of different molecular volumes; $V_{m,A} : V_{m,B} = 1 : 5$. (III) The influence of different molecular volumes and surface; $A_{m,A} : A_{m,B} = 1 : 10$. Dashed curves: Predictions for athermal mixtures ($\chi = 0$) with mixing entropy only. Solid curves: Predictions for the same mixtures with attraction between the different components.

according to the value of the molar volumes used, in such a way that a larger s is obtained when the difference in molar volume between the components of the mixture is larger. For the particular case at hand, this is the estimate resulting from the correlation based on Bondi's estimates [44].

In Fig. 3 panel II the effect of the entropy models on the resulting phase diagrams, assuming zero enthalpy of mixing, is demonstrated. It shows that using the Flory–Huggins entropy in combination with molar van der Waals volumes estimated from the correlation mentioned before [44], results in the largest melting point depression without invoking enthalpic interactions. However, still a significant difference exists when compared to the measured melting point depressions (symbols). Therefore it can be concluded that entropy alone is not enough to explain the observed melting point depressions.

When fitting phase diagrams to experimental data through Eq. (3), the use of different models for the entropy of mixing result in different values for the enthalpies of mixing h , as pictured in Fig. 3 panel III (with the resulting phase diagrams shown in panel IV). It clearly shows that for s^x , where the entropy of mixing is underestimated, the enthalpy of mixing has the largest magnitude, as it needs to compensate to obtain approximately the same Gibbs energy to fit the experimentally obtained phase diagram. This difference in enthalpic contributions is also visible in the interaction parameter χ , listed in Table 2. It shows that for s^x , the interaction parameter χ is

significantly larger in magnitude, almost differing by unity, than when s^ϕ is employed. Also the different molar volumes, s_{Bondi}^ϕ and s_{MMP}^ϕ (based on Bondi and Molecular Modeling Pro, respectively), result in differences in interaction parameters of about 0.2. As expected, applying the Staverman–Guggenheim entropy of mixing does not affect the interaction parameters significantly. The resulting phase diagrams in Fig. 3 panel IV are nearly indistinguishable, which is confirmed by the resulting eutectic temperatures T_e and eutectic composition x_e also listed in Table 2, which do not differ significantly.

The behavior of the other mixtures, succinic acid or pimelic acid with Pe_4NBr , given in Table A1 and shown in Fig. A1 and Fig. A2, is similar and confirms that accounting for volumes according to Flory–Huggins is necessary when the components differ in size. This was already pointed out by Fowler and Guggenheim for $V_{m,1}/V_{m,2} > 2$ [45]. Even though the magnitude of the mixing enthalpy is affected by the choice of specific entropy model, the trends in non-ideality observed earlier [32] are preserved.

3. Conclusions

We have shown that an ideal entropy of mixing underestimates the entropic contribution for mixtures of components often used for DESs. Accounting for volumes of the components according to

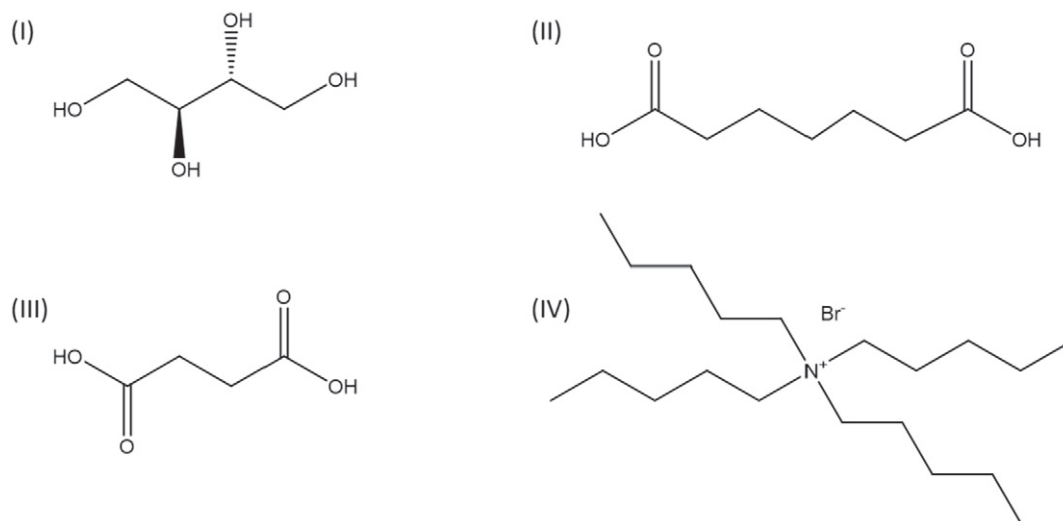


Fig. 2. Molecular structures of the various components studied in this work. (I) Erythritol, (II) pimelic acid, (III) succinic acid, and (IV) tetrapentylammonium bromide (Pe_4NBr).

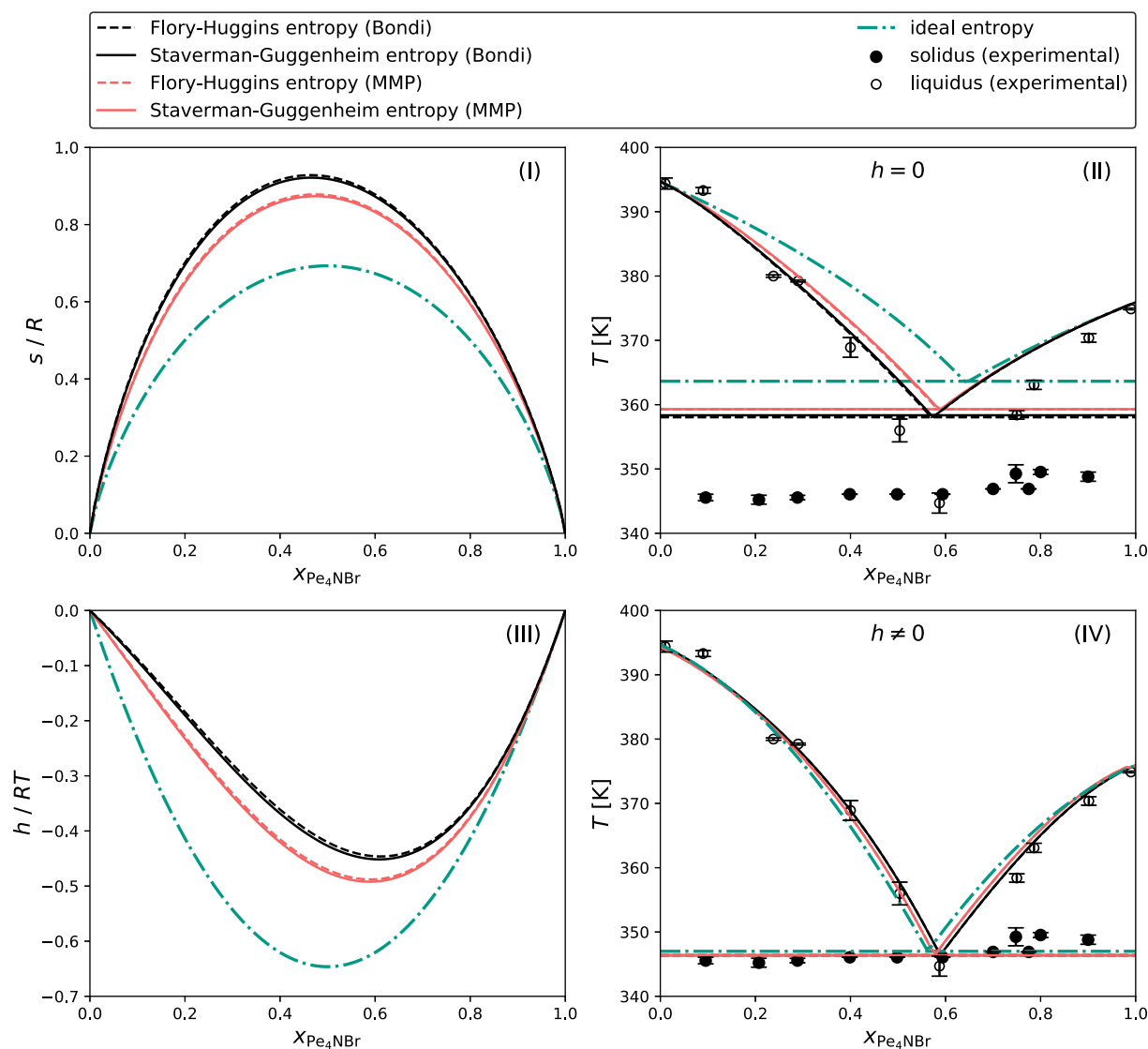


Fig. 3. Diagrams for Pe_4NBr -erythritol describing (I) the entropy of mixing, (II) the melting point depression predicted based on entropy alone ($h = 0$, curves) compared to experimental data (symbols), (III) the enthalpy of mixing obtained after fitting measured melting point depressions, and (IV) the fitted melting point depressions compared to experimental data. Various entropy models are used: ideal, Flory–Huggins, and Staverman–Guggenheim. The latter two are combined with van der Waals volumes and areas estimated using the Molecular Modeling Pro software (MMP) and Bondi’s method. Experimental data taken from Ref. [32].

Flory–Huggins theory is necessary when the components significantly differ in size. Furthermore we demonstrated that extending the theory according to Staverman–Guggenheim is not necessary for the mixtures. The molar volume values employed have a significant influence on the resulting entropy of mixing and therefore on the estimated ideal/reference melting point depression. Both effects result in a significantly different enthalpy of mixing and will thus

affect similarly the interaction parameter χ which we have proposed to use to quantify the non-ideality of DESs and to describe their liquid window. Thus, for a thorough characterization of the behavior of deep eutectic solutions a proper choice of entropy expression and value of molar volume is a prerequisite.

4. Experimental

The experimental data reported here was directly taken from our previous publications [31, 32, 46]. Molar volumes were experimentally obtained by measuring the densities at room temperature using a Micromeritics AccuPyc II 1340 Gas pycnometer. The melting points of the different ratios of the mixtures were measured using melting point capillaries. The DES compositions used were prepared inside a glove-box with dry nitrogen atmosphere, yielding DES mixtures with moisture levels below 10 ppm. The temperature of the first liquid visible at a heating rate of $5 \text{ K} \cdot \text{min}^{-1}$ was taken for the solidus line (eutectic temperature); the temperature at which the last solids were observed to disappear at a heating of $1 \text{ K} \cdot \text{min}^{-1}$ was taken for the liquidus line (melting point).

Table 2

Results of the mixture erythritol with Pe_4NBr . Listed are the theory used for the entropy of mixing s , the interaction parameter χ , p_1 as the second fit parameter [32], the eutectic temperature T_e , the eutectic composition x_e , and the standard error SE between the fit of the phase diagram and the data points.

System	s	χ	p_1	T_e [K]	x_e	SE [K]
Erythritol– Pe_4NBr	s^x	–2.61	0	346.9	0.56	2.5
	s_{Bondi}^{ϕ}	–1.68	–0.88	346.4	0.59	2.0
	s_{Bondi}^{β}	–1.71	–0.87	346.4	0.59	2.0
	s_{MMP}^{ϕ}	–1.88	–0.75	346.4	0.59	2.0
	s_{MMP}^{β}	–1.90	–0.74	346.4	0.59	2.0

The van der Waals volumes V_m and surface areas A_m have been obtained following Bondi based on measured molar volumes, according to Vera et al. [44]:

$$V_m^{\text{Bondi}} = 0.554V_m^{\text{measured}}, \quad (17a)$$

$$A_m^{\text{Bondi}} = 1.323 \times 10^8 \text{ cm}^{-1} V_m^{\text{Bondi}} + 6.259 \times 10^8 \text{ cm}^2 \text{ mol}^{-1}. \quad (17b)$$

Additionally, we estimated the van der Waals volumes and surface areas using Molecular Modeling Pro, ChemSW Inc. (Fairfield, California).

Declaration of competing interest

The authors declare that they have no known competing financial interests or personal relationships that could have appeared to influence the work reported in this paper.

Acknowledgments

GdW and RT acknowledge Gerard Krooshof (DSM) for useful discussions on the thermodynamics of mixtures. The authors would like to thank Marco Hendrix for the experimental support provided, and the members of the ISPT “Deep Eutectic Solvents in the pulp and paper industry” consortium for their financial and in kind contribution. This cluster consists of the following organisations: Altri–Celbi, Buckman, Crown Van Gelder, CTP, DS Smith Paper, ESKA, Essity, Holmen, ISPT, Mayr–Melnhof Eerbeek, Metsä Fibre, Mid Sweden University, Mondi, Omya, Parenco BV, The Navigator Company, Sappi, Essity, Smurfit Kappa, Stora Enso, Eindhoven University of Technology, University of Aveiro, University of Twente, UPM, Valmet Technologies Oy, Voith Paper, VTT Technical Research Centre of Finland Ltd, WEPA and Zellstoff Pöls. Furthermore, this project received funding from the Bio-Based Industries Joint Undertaking under the European Union’s Horizon 2020 research and innovation programme under grant agreement Provides no. 668970. MV acknowledges the Netherlands Organisation for Scientific Research (NWO) for a Veni grant (no. 722.017.005).

Appendix A. Additional results

Table A1

Results for the mixtures of erythritol, succinic acid, and pimelic acid with Pe_4NBr . Listed are the theory used for the entropy of mixing s , the interaction parameter $\chi = p_0$, the second fit parameter p_1 [32], the eutectic temperature T_e , the eutectic composition x_e , and the standard error SE between the fit of the phase diagram and the data points.

System	s	χ	p_1	T_e [K]	x_e	SE [K]
Erythritol– Pe_4NBr	s^x	−2.61	0	346.9	0.56	2.50
	s_{Bondi}^ϕ	−1.68	−0.88	346.4	0.59	1.99
	s_{Bondi}^θ	−1.71	−0.87	346.4	0.59	1.99
	s_{MMP}^ϕ	−1.88	−0.75	346.4	0.59	2.00
	s_{MMP}^θ	−1.90	−0.74	346.4	0.59	2.00
	s^x	−4.86	1.01	349.9	0.65	3.39
Succinic acid– Pe_4NBr	s_{Bondi}^ϕ	−3.93	0	348.3	0.64	3.88
	s_{Bondi}^θ	−3.96	0	348.2	0.64	3.91
	s_{MMP}^ϕ	−4.17	0	347.8	0.64	4.11
	s_{MMP}^θ	−4.18	0	347.8	0.64	4.13
	s^x	−6.40	−2.73	309.6	0.53	1.85
	s_{Bondi}^ϕ	−5.86	−2.93	309.6	0.53	1.90
Pimelic acid– Pe_4NBr	s_{Bondi}^θ	−5.87	−2.93	309.6	0.53	1.90
	s_{MMP}^ϕ	−5.95	−2.88	309.6	0.53	1.88
	s_{MMP}^θ	−5.95	−2.88	309.6	0.53	1.88

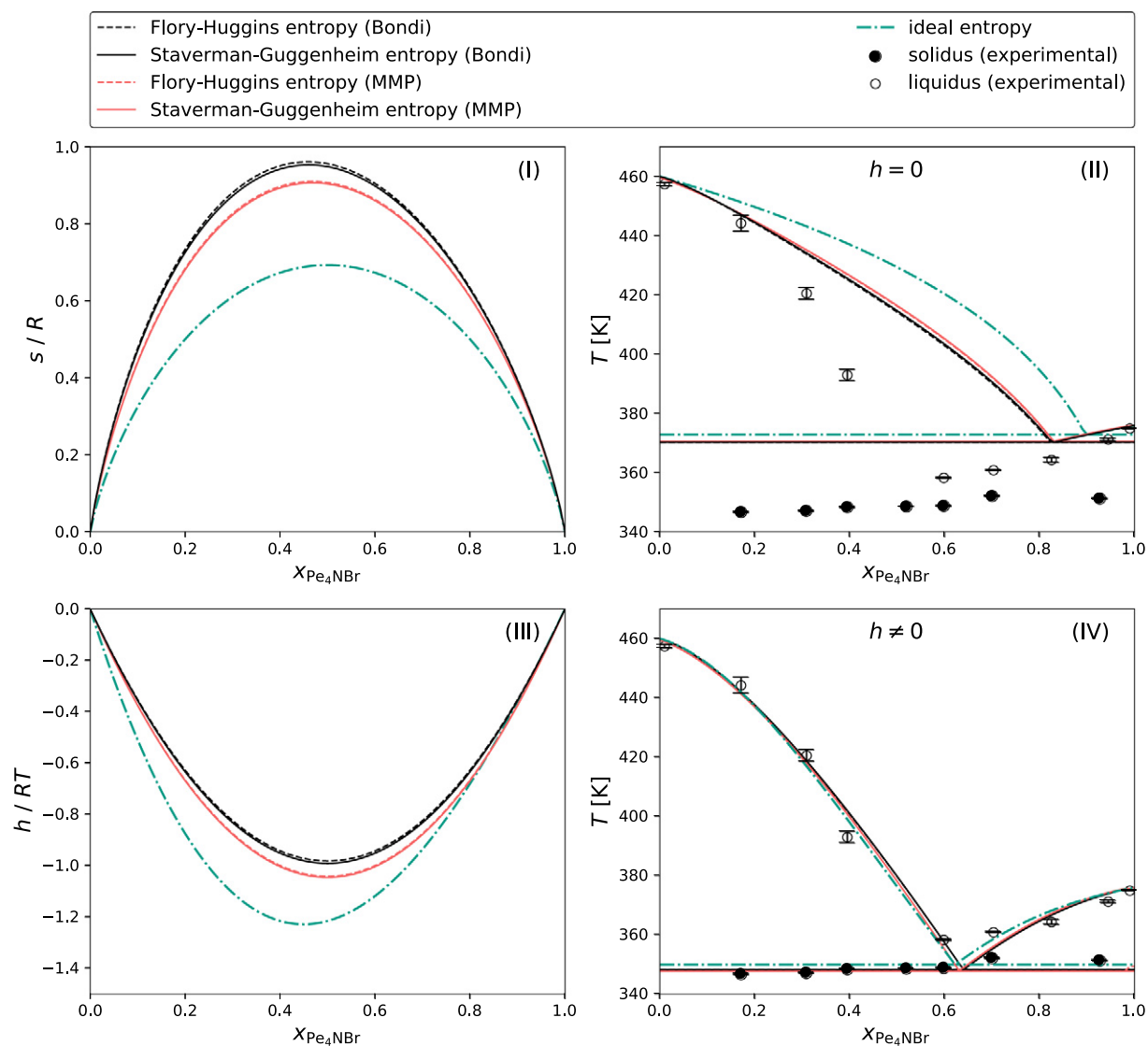


Fig. A1. Diagrams for Pe_4NBr -succinic acid describing (I) the entropy of mixing, (II) the melting point depression predicted based on entropy alone ($h = 0$, curves) compared to experimental data (symbols), (III) the enthalpy of mixing obtained after fitting measured melting point depressions, and (IV) the fitted melting point depressions compared to experimental data. Various entropy models are used: ideal, Flory-Huggins, and Staverman-Guggenheim. The latter two are combined with van der Waals volumes and areas estimated using the Molecular Modeling Pro software (MMP) and Bondi's method. Experimental data taken from Ref. [32].

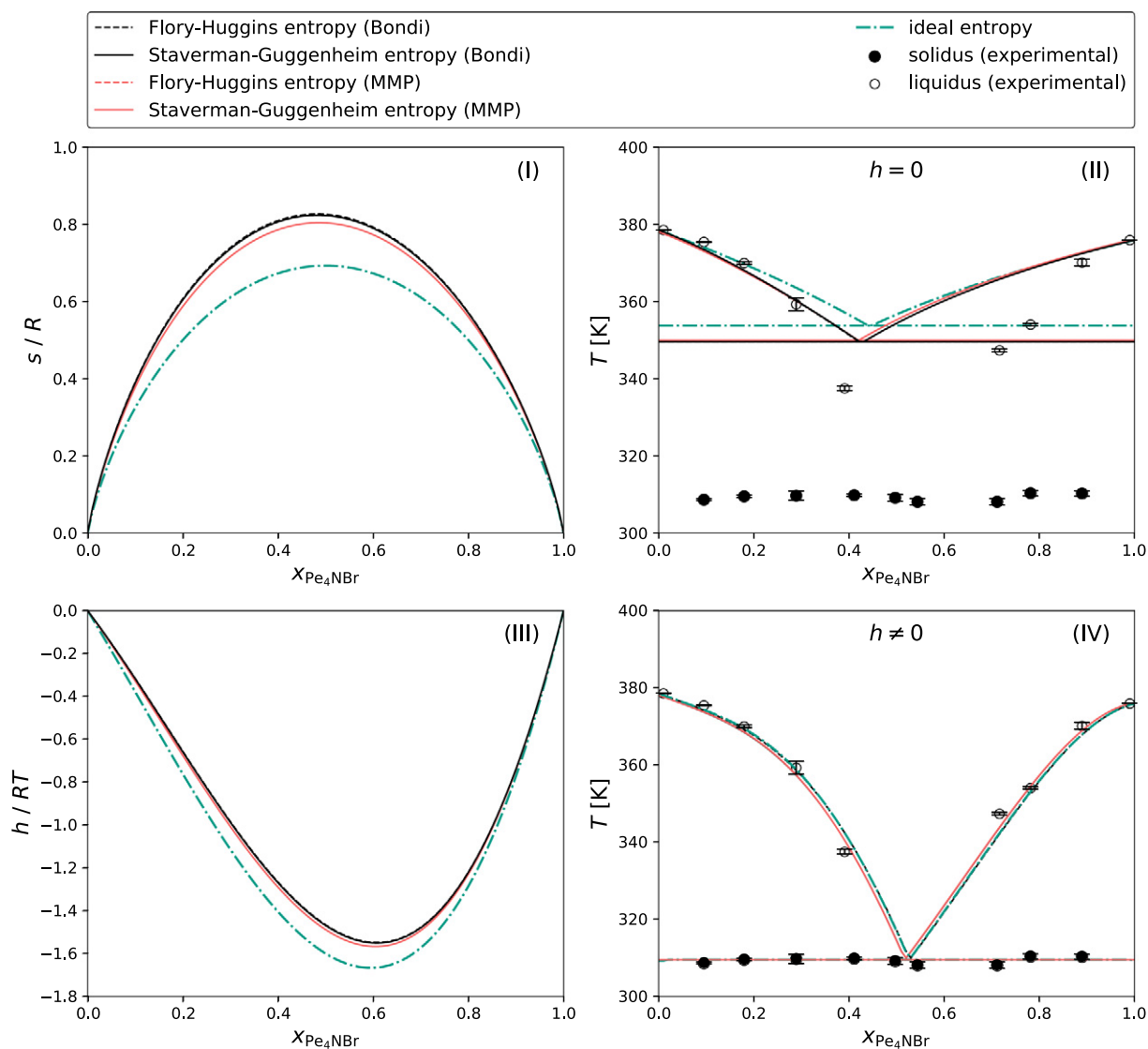


Fig. A2. Diagrams for Pe_4NBr -pimelic acid describing (I) the entropy of mixing, (II) the melting point depression predicted based on entropy alone ($h = 0$, curves) compared to experimental data (symbols), (III) the enthalpy of mixing obtained after fitting measured melting point depressions, and (IV) the fitted melting point depressions compared to experimental data. Various entropy models are used: ideal, Flory–Huggins, and Staverman–Guggenheim. The latter two are combined with van der Waals volumes and areas estimated using the Molecular Modeling Pro software (MMP) and Bondi’s method. Experimental data taken from Ref. [32].

References

- [1] F. Guthrie, On eutexia, *Phys. Soc.* (1884) 462–482.
- [2] F. Guthrie, On salt-solutions and attached water, *Philos. Mag. Ser. 5* 18 (111) (1884) 105–120.
- [3] A.P. Abbott, G. Capper, D.L. Davies, R.K. Rasheed, V. Tambyrajah, Novel solvent properties of choline chloride/urea mixtures, *Chem. Commun.* (2003) 70–71.
- [4] D.J.G.P. van Osch, L.J.B.M. Kollau, A. van den Bruinhorst, S. Asikainen, M.A. Rocha, M.C. Kroon, Ionic liquids and deep eutectic solvents for lignocellulosic biomass fractionation, *Phys. Chem. Chem. Phys.* 19 (2017) 2636–2665.
- [5] M. Zdanowicz, K. Wilpiszewska, T. Szychaj, Deep eutectic solvents for polysaccharides processing. A review, *Carbohydr. Polym.* 200 (2018) 361–380.
- [6] A. Škulcová, L. Kamenská, F. Kalman, A. Ház, M. Jablonský, K. Čížová, I. Šurina, Deep eutectic solvents as medium for pretreatment of biomass, *Key Eng. Mater.* 688 (2016) 17–24.
- [7] K.D.O. Vigier, G. Chatel, F. Jérôme, Contribution of deep eutectic solvents for biomass processing: opportunities, challenges, and limitations, *ChemSusChem* 7 (2015) 1250–1260.
- [8] Y. Zhang, X. Ji, X. Lu, Choline-based deep eutectic solvents for CO_2 separation: review and thermodynamic analysis, *Renew. Sustain. Energy Rev.* 97 (2018) 436–455.
- [9] G. García, M. Atilhan, S. Aparicio, A theoretical study on mitigation of CO_2 through advanced deep eutectic solvents, *Int. J. Greenh. Gas Control* 39 (2015) 62–73.
- [10] D. Carriazo, M.C. Serrano, M.C. Gutiérrez, M.L. Ferrer, F. del Monte, Deep-eutectic solvents playing multiple roles in the synthesis of polymers and related materials, *Chem. Soc. Rev.* 41 (2012) 4996.
- [11] B.Y. Zhao, P. Xu, F.X. Yang, H. Wu, M.H. Zong, W.Y. Lou, Biocompatible deep eutectic solvents based on choline chloride: characterization and application to the extraction of rutin from *Sophora japonica*, *ACS Sustain. Chem. Eng.* 3 (2015) 2746–2755.
- [12] Q. Zhang, K. De Oliveira Vigier, S. Royer, F. Jérôme, Deep eutectic solvents: syntheses, properties and applications, *Chem. Soc. Rev.* 41 (2012) 7108.
- [13] E.L. Smith, A.P. Abbott, K.S. Ryder, Deep eutectic solvents (DESs) and their applications, *Chem. Rev.* 114 (2014) 11060–11082.
- [14] A. Pelczarska, D. Ramjugernath, J. Rarey, U. Domańska, Prediction of the solubility of selected pharmaceuticals in water and alcohols with a group contribution method, *J. Chem. Thermodyn.* 62 (2013) 118–129.
- [15] A. Diedrichs, J. Gmehling, Solubility calculation of active pharmaceutical ingredients in alkanes, alcohols, water and their mixtures using various activity coefficient models, *Ind. Eng. Chem. Res.* 50 (2011) 1757–1769.
- [16] H. Suzuki, H. Sunada, Comparison of nicotinamide, ethylurea, and polyethylene glycole as carriers for nifedipine solid dispersion systems, *Chem. Pharm. Bull.* 45 (1997) 1688–1693.
- [17] I. Pasquali, R. Bettini, F. Giordano, Thermal behaviour of diclofenac, diclofenac sodium and sodium bicarbonate compositions, *J. Therm. Anal. Calorim.* 90 (2007) 903–907.

- [18] C. Herman, B. Haut, L. Aerts, T. Leyssens, Solid-liquid phase diagrams for the determination of the solid state nature of both polymorphs of (RS)-2-(2-oxo-pyrrolidin-1-yl)-butyramide, *Int. J. Pharm.* 437 (2012) 156–161.
- [19] P. Mekala, V. Kamisetty, W.M. Chien, R. Shi, D. Chandra, J. Sangwai, A. Talekar, A. Mishra, Thermodynamic modeling of binary phase diagram of 2-amino-2-methyl-1, 3-propanediol and TRIS(hydroxymethyl)aminomethane system with experimental verification, *CALPHAD Comput. Coupling Phase Diagrams Thermochem.* 50 (2015) 126–133.
- [20] K. Pielichowski, K. Flejtuch, Differential scanning calorimetry study of blends of poly (ethylene glycol) with selected fatty acids, *Macromol. Mater. Eng.* 288 (2003) 259–264.
- [21] E. Palomo Del Barrio, R. Cadoret, J. Daranlot, F. Achchaq, New sugar alcohols mixtures for long-term thermal energy storage applications at temperatures between 70°C and 100°C, *Sol. Energy Mater. Sol. Cells* 155 (2016) 454–468.
- [22] H. Schmit, C. Rathgeber, P. Hennemann, S. Hiebler, Three-step method to determine the eutectic composition of binary and ternary mixtures: tested on two novel eutectic phase change materials based on salt hydrates, *J. Therm. Anal. Calorim.* 117 (2014) 595–602.
- [23] B. He, V. Martin, F. Setterwall, Liquid-solid phase equilibrium study of tetradecane and hexadecane binary mixtures as phase change materials (PCMs) for comfort cooling storage, *Fluid Phase Equilib.* 212 (2003) 97–109.
- [24] D. Wei, S. Han, B. Wang, Solid-liquid phase equilibrium study of binary mixtures of n-octadecane with capric, and lauric acid as phase change materials (PCMs), *Fluid Phase Equilib.* 373 (2014) 84–88.
- [25] P. Zhao, Q. Yue, H. He, B. Gao, Y. Wang, Q. Li, Study on phase diagram of fatty acids mixtures to determine eutectic temperatures and the corresponding mixing proportions, *Appl. Energy* 115 (2014) 483–490.
- [26] G. Diarce, L. Quant, Á. Campos-Celador, J. Sala, A. García-Romero, Determination of the phase diagram and main thermophysical properties of the Erythritol-Urea eutectic mixture for its use as a phase change material, *Sol. Energy Mater. Sol. Cells* 157 (2016) 894–906.
- [27] A.E. Hoyt, S.J. Huang, Binary mixtures of liquid crystalline ester bismaleimides, *J. Macromol. Sci. Part A* 32 (1995) 1931–1945.
- [28] G.W. Smith, The influence of a metastable solid phase on eutectic formation of a binary nematic liquid crystal, *Mol. Cryst. Liq. Cryst.* 30 (1975) 101–107.
- [29] R.I. Nessim, Applicability of the Schröder-van Laar relation to multi-mixtures of liquid crystals of the phenyl benzoate type, *Thermochim. Acta* 343 (2000) 1–6.
- [30] M. Sato, T. Nakano, K.I. Mukaida, Side-chain liquid crystalline homo-and copolymeracrylates with a carbonate linkage between the benzylideneaniline mesogen and ethylene chain, *Liq. Cryst.* 18 (1995) 645–649.
- [31] L.J.B.M. Kollau, M. Vis, A. van den Bruinhorst, A.C.C. Esteves, R. Tuinier, Quantification of the liquid window of deep eutectic solvents, *Chem. Commun.* 54 (2018) 13351–13354.
- [32] L.J.B.M. Kollau, M. Vis, A. van den Bruinhorst, G. de With, R. Tuinier, Activity modelling of the solid-liquid equilibrium of deep eutectic solvents, *Pure Appl. Chem.* 91 (2019) 1341–1349.
- [33] O. Redlich, A.T. Kister, On the thermodynamics of non-electrolyte solutions and its technical applications: III. Systems with associated components, *J. Chem. Phys.* 15 (1947) 849–855.
- [34] O. Redlich, A.T. Kister, Thermodynamics of nonelectrolyte solutions - x-y-t relations in a binary system, *Ind. Eng. Chem.* 40 (1948) 341–345.
- [35] A.D. Pelton, C.W. Bale, Legendre polynomial expansions of thermodynamic properties of binary solutions, *Metall. Trans. A* 17 (1986) 1057–1063.
- [36] C.J. Van Tyne, P.M. Novotny, S.K. Tarby, Solution thermodynamic quantities represented by modified legendre polynomials, *Metall. Trans. B* 7 (1976) 299–300.
- [37] Z. Bouzina, M.R. Mahi, I. Mokbel, A. Negadi, C. Gouthaudier, J. Jose, L. Negadi, Vapour-liquid equilibria, enthalpy of vaporisation, and excess Gibbs energies of binary mixtures of 3,3-diamino-N-methyldipropylamine (DNM) (or N,N,N',N"-pentamethyldiethylenetriamine (PMDETA))+water, *J. Chem. Thermodyn.* 128 (2019) 251–258.
- [38] I. Díaz, M. Rodríguez, E.J. González, M. González-Miquel, A simple and reliable procedure to accurately estimate NRTL interaction parameters from liquid-liquid equilibrium data, *Chem. Eng. Sci.* 193 (2019) 370–378.
- [39] C. Du, R. Dong, B. Qiao, Z. Jin, T. Ye, Y. Zhang, M. Wang, Construction and evaluation of ternary solid-liquid phase diagram of pyraclostrobin (form IV) and its intermediate in ethanol and N,N-dimethylformamide, *J. Chem. Thermodyn.* 128 (2019) 1–9.
- [40] H. Renon, J.M. Prausnitz, Local compositions in thermodynamic excess functions for liquids mixtures, *AIChE J.* 14 (1968) 116–128.
- [41] G.J. Krooshof, R. Tuinier, G. de With, On the calculation of nearest neighbors in activity coefficient models, *Fluid Phase Equilib.* 465 (2018) 10–23.
- [42] E.A. Guggenheim, Statistical thermodynamics of co-operative systems (a generalization of the quasi-chemical method), *Trans. Faraday Soc.* 44 (1948) 1007–1012.
- [43] A.J. Staverman, The entropy of high polymer solutions., *Recl. Trav. Chim. Pays-Bas* 69 (1950) 163–174.
- [44] J.H. Vera, S.G. Sayegh, G.A. Ratcliff, A quasi lattice-local composition model for the excess Gibbs free energy of liquid mixtures, *Fluid Phase Equilib.* 1 (1977) 113–135.
- [45] R.H. Fowler, E.A. Guggenheim, *Statistical Thermodynamics*, Cambridge University Press, Cambridge, 1939.
- [46] L.J.B.M. Kollau, On the description, quantification, and prediction of deep eutectic mixtures, PhD thesis. Eindhoven University of Technology, 2019. link: <https://research.tue.nl/en/publications/on-the-description-quantification-andprediction-of-deep-eutectic>.